New Adsorbents for Purification: Selective Removal of Aromatics

Akira Takahashi and Ralph T. Yang
Dept. of Chemical Engineering, University of Michigan, Ann Arbor, MI 48109

Adsorption of benzene and cyclohexane on various Y-zeolites was investigated to develop sorbents for the purification of aliphatics by removal of aromatics. Ag-Y showed superior benzene/cyclohexane selectivities to Na-Y, Pd-Y, and H-USY. Separation factors greater than 10^5 were obtained with Ag-Y at low concentrations of benzene. High selectivities were achieved by the strong interaction between benzene and Ag-Y, while the interaction with cyclohexane was not influenced by the cations. Molecular orbital calculation revealed that benzene formed a classic π-complexation bond with Ag-Y: donation of electron charges from the p-orbitals of benzene to the vacant s-orbital of the silver (σ donation) and, simultaneously, back donation of electron charges from d-orbitals of silver to π^*-orbital of benzene ($d-\pi^*$ back donation). Grand canonical Monte Carlo simulations were also performed for adsorption isotherms. Potential parameters of benzene on Ag-Y, including π-complexation, were developed first. Simulation and experiments of GCMC agreed excellently for adsorption of benzene on Y-zeolites.

Introduction

Purification of aliphatics by removing aromatics is important in both the petrochemical industry and for pollution control. Because benzene (and aromatics) is known to be highly carcinogenic, the concentration of benzene needs to be minimized in automotive fuel. A number of separation processes have been employed to reduce the benzene concentration in a refinery's gasoline pool, so that it meets new reformulated gasoline requirements. In a typical benzene-reduction process, a combination of extraction and distillation is used (Jeanneret, 1997). Also, removal of aromatics from kerosene improves the clean burning properties of the fuel and separation of the aromatics from the isoparaffins and naphthenes in lubricating oils improves the viscosity–temperature relationship (Bailes, 1983).

Because of the importance of aromatics/aliphatics separation and the problems associated with current separation processes, possible alternatives have been under continuing investigation. These include pervaporation (Hao et al., 1997), liquid membranes (Li, 1968), and the use of liquid inclusion complexes (Atwood, 1984). Purification of dilute aromatics from aliphatics (e.g., toluene and/or xylene in heptane) by temperature swing adsorption (TSA) was studied in the liquid phase (Matz and Knaebel, 1990). Commercially available sorbents were used: silica gel, activated alumina, activated carbon, zeolite 13X, and polymeric resin (XAD-7). Among these sorbents, silica gel was considered the best due to its superior thermal-exchange capacity. However, the selectivities were low.

Adsorption plays an increasingly important role in separations. However, its utility is limited by the availability of selective sorbents. The conventional sorbents and separations using them are based on van der Waals and electrostatic interactions between the sorbate and the sorbent. Studies of new sorbents using weak chemical bonds such as chemical complexation have begun only recently in our laboratory. As suggested by King (1987), chemical complexation bonds are generally stronger than van der Waals interactions, yet weak enough to be reversible. Therefore, tremendous opportunities exist for developing new sorbents and new applications in separations by using weak chemical bonds, including various forms of complexation bonds.

The π-complexation is a subclass of chemical complexation. It pertains to the main group (or d-block) transition

Correspondence concerning this article should be addressed to R. T. Yang.

metals, that is, from Sc to Cu, Y to Ag, and La to Au in the periodic table (Cotton and Wilkinson, 1966). These metals or their ions can form the normal σ-bond to carbon and, in addition, the unique characteristics of the d-orbitals in these metals or ions can form bonds with unsaturated hydrocarbons in a nonclassic manner. This type of bonding is broadly referred to as π-complexation. This π-complexation has been seriously considered for olefin/paraffin separations using liquid solutions containing silver or cuprous ions (Quinn, 1971; Ho et al., 1988; Keller et al., 1992; Blytas, 1992; Eldridge, 1993; Safarik and Eldridge, 1988). These involved gas–liquid operations. While gas–solid operation can be simpler as well as more efficient, particularly by pressure swing adsorption, the list of attempts for developing solid π-complexation sorbent is a short one.

More recently, several new sorbents based on π-complexation were prepared for selective olefin adsorption. These included Ag^+-exchanged resins (Yang and Kikkinides, 1995; Wu et al., 1997), monolayer CuCl on pillared clays (Cheng and Yang, 1995), and monolayer $AgNO_3/SiO_2$ (Padin and Yang, 1997; Rege et al., 1998; Padin and Yang, 2000). Moreover, Ag ion-exchanged Y-zeolite was developed to purify butene by removing trace amounts of butadiene (Padin et al., 1999). The purification performance of this sorbent was superior to that of NaY owing to π-complexation.

It is possible, in principle, to purify aromatics from aliphatics based on π-complexation. In the benzene molecules, the carbon atom is sp^2 hybridized. Hence, each carbon has three sp^2-orbitals and another P_Z-orbital. The six P_Z-orbitals in the benzene ring form the conjugative π bonds. The P_Z-orbitals also form the antibonding π^*-orbitals, which are not occupied. When benzene interacts with transition metals, the π^*-orbitals of benzene could overlap with the empty or unfilled outer shell s-orbital of the transition metal to form a σ-bond. Furthermore, the vacant antibonding π^*-orbitals of benzene could overlap with the d-orbitals in the transition metals, like that formed in the olefin–Cu^+ bond (Huang et al., 1999a). In this work, Ag^+ and Pd^{2+} ion-exchanged zeolites were selected for the study of aromatics/aliphatics separations, since these two cations have the most promising π-complexation capabilities and they are stable. In order to understand the effects of π-complexation, Ag^+ and Pd^{2+} ion-exchanged zeolites were compared with that of Na^+ ion-exchanged zeolite and a high-SiO_2 zeolite.

Benzene and cyclohexane are an ideal pair of model compounds for studying selective sorbents for purification. These molecules have similar shapes, polarizabilities, and volatilities (the boiling points are 80°C for benzene and 81°C for cyclohexane). The kinetic diameter of benzene, which is calculated from the minimum equilibrium cross-sectional diameter, is estimated to be 5.85 Å compared with 6.0 Å for cyclohexane (Breck, 1974). Therefore, benzene and cyclohexane were used in this work.

In addition to the experimental investigation, molecular orbital calculations were performed to obtain a basic understanding of the origin of the strong interactions of Ag ion-exchanged zeolite with benzene. Moreover, grand canonical Monte Carlo (GCMC) simulations were used to simulate/predict the isotherms. Many GCMC studies have been performed for predicting adsorption isotherms in zeolites. These include N_2, O_2, Ar, Xe, CH_4, C_2H_4, and C_4H_{10} on zeolite-A,-X,-Y, and MFI-type zeolite (Woods and Rowlinson, 1989; Razmus and Hall, 1991; Kravias and Myers, 1991; Watanabe et al., 1995). Adsorption of benzene on NaY, Heulandite, and MFI-type zeolites has also been studied (Snurr et al., 1994; Kitagawa et al., 1996; Klemm et al., 1998; Laboy et al., 1999). However, these studies did not involve the effects of π-complexation on adsorption. In this study, benzene adsorption isotherms on Ag ion-exchanged Y-zeolite were simulated.

Experimental Details

Sorbent preparation

The sorbents in this work were ion-exchanged zeolites. From earlier results on olefin/paraffin separations (Yang and Kikkinides, 1995; Wu et al., 1997; Cheng and Yang, 1995; Padin and Yang, 1997, 2000; Rege et al., 1998), Ag^+ and Pd^{2+} were the most promising ions because of their strong π-complexation abilities.

Ion-exchange of zeolites was accomplished with aqueous solutions. Faujasite was selected as the zeolite framework structure for ion-exchange because of its large-pore aperture (7.4 Å), large-pore volume (0.489 mL/mL), and wide range of SiO_2/Al_2O_3 ratios (1–∞). Two as-received zeolites, Na-type Y-zeolite (Na-Y, Si/Al = 2.43, Strem Chemical), and H-type ultrastable Y-zeolite (H-USY, Si/Al = 195, Tosoh Corporation, HSZ-390HUA), were used in this study. The Pd^{2+}-type Y-zeolite was prepared by exchanging Na-Y zeolite with $Pd(NO_3)_2$ (Aldrich) in an aqueous solution (Li and Armor, 1994). First, Na-Y was exchanged using 2-fold excess of $Pd(NO_3)_2$ (0.005 M) at 80°C for 24 h. After the exchange, the zeolite suspension was filtered and washed with a copious amount of deionized water. The product was dried at 110°C overnight in air. The Ag^+ ion exchange was prepared at room temperature for 24 h in the same manner as Pd^{2+} exchange, using 2-fold excess $AgNO_3$ (0.1 M).

Adsorption isotherms and uptake rates

Single-component isotherms for benzene and cyclohexane were measured using standard gravimetric methods. A Shimadzu TGA-50 automatic recording microbalance was employed. Helium (prepurified grade, Metro Welding, 99.995%) was used as the carrier gas and was first passed through two consecutive gas-wash bottles (to ensure saturation) that contained benzene (HPLC grade, Sigma-Aldrich, 99.9+%) or cyclohexane (HPLC grade, Aldrich, 99.9+%). After diluting the concentration to the desired value by blending with additional helium (total flow rate: 250 cc/min), the mixture was directed into the microbalance.

Isosteric heats of adsorption were calculated using the Clausius–Clapeyron equation from isotherms at different temperatures. Nitrogen isotherms at 77 K measured with a Micromeritics ASAP 2010 system were used for pore-size distribution and pore-volume determination. Pore-size distributions were calculated with the Horvath–Kawazoe equation (Horvath and Kawazoe, 1983; Cheng and Yang, 1994). Pore volumes were calculated at 0.95 P/Po. The overall diffusion time constants, D/r^2, were calculated from the uptake rates (Yeh, 1989). In this work, the short time region was used.

Molecular Orbital Calculation Details

The π-complexation bonding between olefins and sorbents have been extensively investigated using molecular orbital (MO) calculations (Chen and Yang, 1996; Huang et al., 1999a, 1999b). More recently, MO studies were extended to benzene adsorption on various salts, such as CuCl and AgCl (Takahashi et al., 2000). In this work, similar MO studies for benzene adsorption on Ag ion-exchanged zeolite were performed using a cluster model of Ag-zeolite. The Gaussian 94 Progam (Frisch et al., 1995) in Cerius2 molecular modeling software (Bowie, 1995) from Molecular Simulation, Inc., was used for calculations. MO calculations for benzene and Ag zeolite were performed at the Hartree-Fock (HF) and density functional theory (DFT) level. The 3-21G basis set is the split-valence basis set, which has been used successfully for many simulations for benzene adsorption on zeolites (O'Malley and Braithwaite, 1995), protonation reaction of propylene and isobutene on zeolite (Viruera-Martin et al., 1993), and O_2, N_2 and C_2H_4 adsorption on Ag-Zeolites (Chen and Yang, 1996). The reliability of this basis set has been confirmed by the accuracy of calculation results in comparison with experimental data. Therefore, the 3-21G basis set was employed for both geometry optimization and natural bond orbital (NBO) analysis.

Geometry optimization and energy of adsorption calculations

The restricted Hartree-Fock (RHF) theory at the 3-21G level basis set was used to determine the geometries and the bonding energies of benzene on the Ag zeolite cluster, since Ag^+ has filled d-orbitals with spin = 1.

The computational model used for Ag zeolite was the same as that used by Chen and Yang (1996), since this model yielded heats of adsorption of N_2 and C_2H_4 on Ag zeolite that agreed well with experimental data. The simplest cluster model, $(HO)_3Si\text{-}O(Ag)\text{-}Al(OH)_3$, was chosen for this work. The optimized structures were then used for bond energy calculations according to the following expression:

$$E_{\text{ads}} = E_{\text{adsorbate}} + E_{\text{adsorbent}} - E_{\text{adsorbent-adsorbate}}, \qquad (1)$$

where $E_{\text{adsorbate}}$ is the total energy of benzene, $E_{\text{adsorbent}}$ is the total energy of the bare adsorbent, that is, the Ag zeolite cluster, and $E_{\text{adsorbent-adsorbate}}$ is the total energy of the adsorbate/adsorbent system.

Natural bond orbital (NBO) analysis

The optimized structures were also used for NBO analysis at the B3LYP/3-21G level. The B3LYP (Becke, 1993a) approach is one of the most useful self-consistent hybrid (SCH) approaches (Becke, 1993b), which is Becke's 3-parameter nonlocal exchange functional (Becke, 1992) with the nonlocal correlation functional of Lee et al. (1988).

The NBO analysis performs population analysis pertaining to the localized wave-function properties. It gives a better description of the electron distribution in compounds of high ionic character, such as those containing metal atoms (Reed et al., 1985). It is known to be sensitive for calculating localized weak interactions, such as charge transfer, hydrogen bonding, and weak chemisorption. Therefore, the NBO program (Glendening et al., 1995) was used for studying the electron density distribution of the adsorption system.

Monte Carlo Simulation Details

Grand canonical ensemble (at a fixed pressure) Monte Carlo simulation was performed utilizing the Cerius2 molecular modeling software (Bowie, 1995) on a Silicon Graphics Indigo2 workstation running IRIX v.6.5. After the "crystal builder" module was used to set up the zeolite models, energy expressions and parameters for force field were input by the "force field editor" module. The "sorption" module was then used for benzene adsorption simulations.

The simulation was performed at 120°C and 180°C for at least 1,000,000 configurations. During the simulation, the sorbate molecules interacted with the potential field generated by sorbate–sorbent and sorbate–sorbate interactions. The initial configurations contained no sorbate molecules. Each subsequent configuration was generated by one of four moves: Create, Destroy, Translate, and Rotate. Molecular creation attempts were made at random points within the accessible portion of the zeolite lattice with the criterion that there be no overlapping sites (i.e., creations that result in interaction sites that were closer than half the sum of the van der Waal's radii of the two sites were rejected). Translation and rotation were performed with the same rejection criterion. For nonoverlapping sites, the change in the potential energy accompanying the new configuration was calculated and subsequently accepted or rejected in accordance with standard acceptance probabilities (Molecular Simulation Inc., 1998).

Zeolite models

The structure determined from powder neutron diffraction data by Fitch et al. (1986) was used as the structure for Na-Y zeolite (Si/Al = 2.43). The location of the Na cations were 32 atoms on SII sites, 16 atoms on SI sites, and 8 atoms on SI′ sites. Na cations on SI and SI′ sites were located in such a manner that two adjacent SI and SI′ sites were not simultaneously occupied. This is due to the electrostatic repulsion caused by their small separation of 0.218 nm (Fitch et al., 1986). The position of Al in the framework was randomly chosen using the "disorder" function in the "crystal builder" module that obeyed the Loewenstein rule. No charge-free "blocking atom" was added because large molecules such as benzene were not located in the site, which was actually sterically inaccessible.

For the simulation of Ag ion-exchanged zeolite (Si/Al = 2.43), the Na cations in Na-Y were replaced by Ag maintaining the same cation locations. An all-silica Y-zeolite structure was used to simulate ultrastable Y-zeolite (Si/Al = 195), since this zeolite has less than one Al atom per unit cell.

Until recently, the location of the Ag cation had not been accurately determined. Using neutron diffraction data, Hutson et al. (2000) reported the Ag location and occupancies of Ag in Ag-Y (Si/Al = 2.43) after 450°C dehydration. Their results showed that the Ag cation sites were 28 atoms on the SII sites, 4 atoms on the SII′ site, 11 atoms on the SI sites, and 12 atoms on the SI′ sites. Simultaneous occupancy of Ag cations at SII and SII′ as well as SI and SI′ sites was unlikely

due to the large repulsion. This location is very similar to the location of Na cations in Na-Y reported by Fitch et al. (1986). Therefore, it is considered that the zeolite model for Ag-Y used in this work reflects the actual Ag cation locations in Ag-Y (Si/Al = 2.43).

Forcefield determination

One of the most important factors for GCMC simulation is the selection of an energy expression and parameters for the force field. The force field used in these simulations was a modified version of Cerius2 Sorption Demontis Force Field, since Demontis et al. simulated the mobility of benzene in Na-Y zeolite successfully using molecular dynamics methods (Demontis et al., 1989). In this model, the total potential energy (U_{Total}) between the zeolite lattice and adsorbate molecules is written as the sum of the interactions between adsorbate molecules (AA) and that between the adsorbate molecules and the zeolite lattice (AZ)

$$U_{\text{total}} = U_{AA} + U_{AZ} \tag{2}$$

Interactions between adsorbate molecules (U_{AA}) were described as the sum of the atom−atom Buckingham potentials (the first and second terms in Eq. 3), which have been shown to yield reasonable predictions for liquid and solid benzene (Williams and Cox, 1984), and the Coulomb interaction potentials (the third term in Eq. 3)

$$U_{ij} = A_{ij} \exp\left(-B_{ij} r_{ij}\right) - \frac{C_{ij}}{r_{ij}^6} + \left(\frac{q_i q_j}{r_{ij}}\right). \tag{3}$$

The first and second terms represent, respectively, the repulsive and dispersive potential energies between sites i and j, and the third term represents the interaction potential between point charges q_i and q_j of sites i and j separated by a distance r_{ij}.

The interactions between the adsorbate molecules and the zeolite lattice (U_{AZ}) is written as the sum of the atom−atom Lennard-Jones 12-6 potential and the Coulomb interaction potentials

$$U_{ij} = 4\epsilon_{ij}\left[\left(\frac{\sigma_{ij}}{r_{ij}}\right)^{12} - \left(\frac{\sigma_{ij}}{r_{ij}}\right)^{6}\right] + \left(\frac{q_i q_j}{r_{ij}}\right). \tag{4}$$

Following the empirical approach used by Razmus and Hall (Razmus and Hall, 1991), Watanabe et al. (Watanabe et al., 1995) used the empirical approach to parameterize the force field for adsorption of N_2, O_2, and Ar in type A and faujasite zeolites. The dispersive part of the Lennard-Jones 12-6 potential ($U_{\text{dispersion}}$) was written using an adjustable parameter (β_i) of the adsorbate and the polarizabilities (α) of the atoms of the adsorbate molecules (i) and in the zeolite lattice (j)

$$U_{\text{dispersion}} = -\beta_i\left(\frac{\alpha_i \alpha_j}{r_{ij}^6}\right). \tag{5}$$

The potential-energy well-depth parameter, ϵ_{ij} ,is then written as

$$\epsilon_{ij} = \beta_i\left(\frac{\alpha_i \alpha_j}{4\sigma_{ij}^6}\right). \tag{6}$$

The Lennard-Jones parameter, σ_{ij}, for the adsorbate-zeolite interaction is given by the mixing rule:

$$\sigma_{ij} = \left(\frac{\sigma_i + \sigma_j}{2}\right) \tag{7}$$

The σ_j for the zeolite lattice are related to the van der Waals radii, R_j, of the respective ions by

$$R_j = 2^{1/6}\sigma_j. \tag{8}$$

Table 1. Potential Parameters Used for Na-Y, Ag-Y, and H-USY

Na-Y	U_{AA}*		C−C	H−H	C−H	
		A (kcal/mol)	88,371	2,861	15,901	
		B (1/A)	3.60	3.74	3.67	
		C (A^{6*} kcal/mol)	583.13	32.60	137.88	
	U_{AZ}		O−C	O−H	Na−C	Na−H
		ϵ (kcal/mol)	0.25547	0.16515	0.04187	0.03153
		σ (A)	2.9984	2.5893	3.3279	2.7651
Ag-Y	U_{AZ}		O−C	O−H	Ag−C	Ag−H
(Case I)		ϵ (kcal/mol)	0.25547	0.16515	***0.7823*****	***0.5895***
		σ (A)	2.9984	2.5893	***3.5773***	***3.0145***
Ag-Y	U_{AZ}		O−C	O−H	Ag−C	Ag−H
(Case II)		ϵ (kcal/mol)	0.25547	0.16515	***0.7601***	***0.5728***
		σ (A)	2.9984	2.5893	***3.5773***	***3.0145***
H-USY	U_{AZ}		O−C	O−H		
		ϵ (kcal/mol)	***0.1687***	***0.1271***		
		σ (A)	2.9984	2.5893		

*Parameters for U_{AA} are the same for all sorbents.
**The boldface italic numbers were determined in this work.

The well-depth parameter, ϵ_{ij}, is assumed to be a geometric combination of ϵ_i and ϵ_j,

$$\epsilon_{ij} = (\epsilon_i \epsilon_j)^{0.5}. \quad (9)$$

The van der Waals energy in the periodic framework was calculated using a minimum image convention with an interaction cutoff distance of 1 nm. The Coulomb term was evaluated using the Evald summation method (Allen and Tildesley, 1987).

The potential parameters used for Na-Y, Ag-Y, and H-USY are listed in Table 1. The potential parameters for Na-Y are the same as that of Demontis et al. (1989). Van der Waals interactions between the adsorbate and zeolite cage were modeled by means of interactions between the (C,H) and (Na,O) atoms. Interactions with the Si and Al atoms were neglected because they were well shielded by the oxygen atoms of the SiO_4 and AlO_4 tetrahedra. Electrostatic interactions between all charges were included in the potential energy calculation. As for Ag-Y and all silica Y zeolites, modification of parameters was performed using the mixing rule and the geometric combination rule. The detailed scheme for parameterization will be discussed shortly.

Assignment of charges for adsorbate and adsorbent

Assignment of charges also has a significant impact on simulation results when the Coulombic interactions are not negligible. In this work, the existing model for benzene in Cerius2 was used. In this model, each carbon in benzene carries a -0.093 point charge, while hydrogen carries a $+0.093$ point charge. These values were nearly the average values from the various charge-determination methods: MOPAC (0.1022), ZINDO (0.072), and the charge equilibration method (Q_{eq}) by Rappe and Goddard (0.1147) (Rappe and Goddard, 1991).

The point charges of zeolite were assigned either by (1) using the point charges in the literature or (2) calculating by means of the charge equilibration method in the Cerius2 software. In this work, Na, Si/Al, O in Na-Y carried the charges of $+0.78$, $+1.2125$, and -0.72, respectively, since these values were successfully used in quantum mechanics simulations (Kitagawa et al., 1996). Here, no distinction was made between Si and Al atoms in terms of point charges. Charges of Ag-Y and all-silica Y-zeolites were calculated by the charge equilibration method: Ag($+0.45$), Si/Al($+1.16875$), O(-0.65), which will be referred to as Case I for Ag-Y, and Si($+1.2650$), O(-0.6325) for H-USY. In order to investigate the effect of the assigned charges to the isotherm simulation results, the same charges that were used for Na-Y, that is, Ag($+0.78$), Si/Al($+1.2125$), and O(-0.72), were also used for Ag-Y. This case is referred to as Case II for Ag-Y. For all cases, regardless of the positions of cations and framework atoms (Si, Al, O), the same values of point charge were assigned to the same atoms throughout the simulation unit cell, even though the point charge might vary with the position of the atom. The Ag cation charges used for Monte Carlo simulation were also consistent with the values calculated by molecular orbital method at MP2/3-21G (Ag charge: $+0.49$) or MP2/LanL2DZ level (Ag charge: $+0.74$) using the zeolite cluster model (Chen and Yang, 1996).

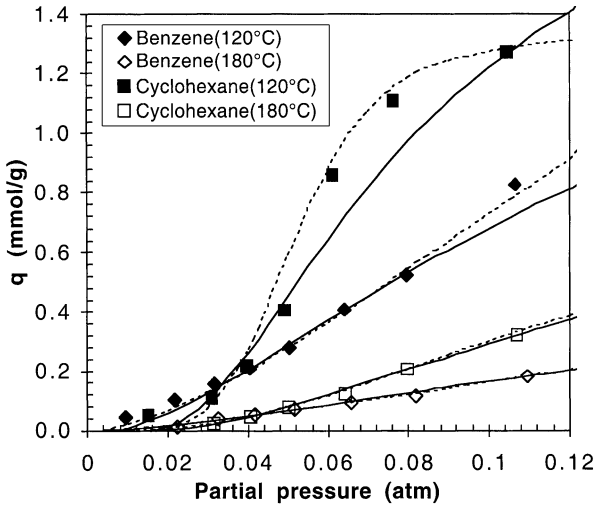

Figure 1. Pure-component equilibrium isotherms for benzene and cyclohexane adsorption on H-USY at 120° and 180°C.

Curves are fitted with Dubinin–Astakhov (solid lines) and Langmuir–Freundlich (dotted lines) isotherms.

Results and Discussion

Experimental studies

Benzene/Cyclohexane Adsorption Isotherms. Pure-component isotherms of benzene and cyclohexane were measured for H-USY(Si/Al = 195), Na-Y(Si/Al = 2.43), Ag-Y(Si/Al = 2.43), and Pd-Y(Si/Al = 2.43) at 120° and 180°C, shown in Figures 1–4. Isosteric heats of adsorption calculated using the Clausius–Clapeyron equation are listed in Table 2.

In the case of H-USY, the adsorbed amounts of cyclohexane were higher than that of benzene at > 0.04 atmosphere.

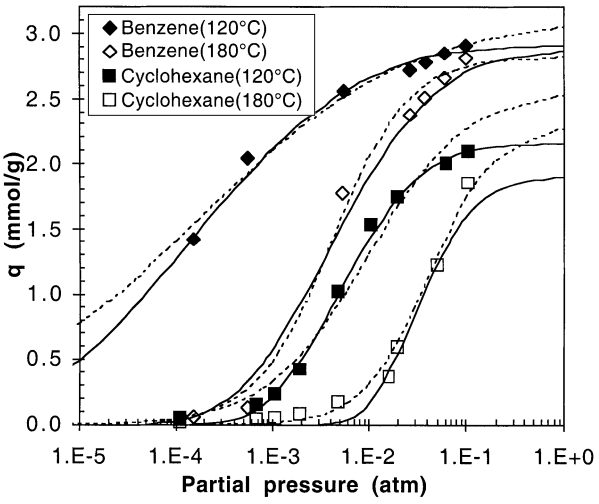

Figure 2. Pure-component equilibrium isotherms for benzene and cyclohexane adsorption on Na-Y at 120° and 180°C.

Curves are fitted with Dubinin–Astakhov (solid lines) and Langmuir–Freundlich (dotted lines) isotherms.

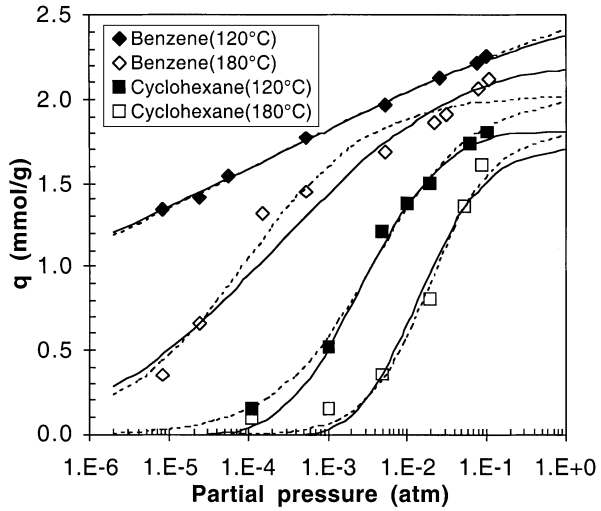

Figure 3. Pure-component equilibrium isotherms for benzene and cyclohexane adsorption on Ag-Y at 120° and 180°C.

Curves are fitted with Dubinin–Astakhov (solid lines) and Langmuir–Freundlich (dotted lines) isotherms.

This result qualitatively agreed with calculations using the Horvath–Kawazoe (H–K) theory (Horvath and Kawazoe, 1983; Cheng and Yang, 1994). The threshold pore-filling vapor pressures of cyclohexane and benzene at 120° and 180°C were calculated using the spherical pore model of the H–K method. The threshold pressure is the pressure where the steep rise in the isotherm occurs. At both temperatures, it was found that the pore-filling pressure of cyclohexane was 20% lower than that of benzene. The reason for this difference was the larger polarizability (11.0×10^{-24} cm^3 for cyclohexane and 10.3×10^{-24} cm^3 for benzene) and magnetic susceptibility (11.3×10^{-29} cm^3 for cyclohexane and 9.1×10^{-29} cm^3 for benzene) of cyclohexane. However, the calculated

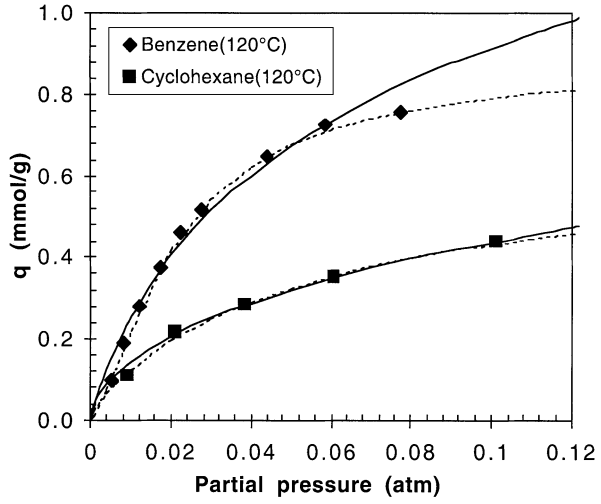

Figure 4. Pure-component equilibrium isotherms for benzene and cyclohexane adsorption on Pd-Y at 120°C.

Curves are fitted with Dubinin–Astakhov (solid lines) and Langmuir–Freundlich (dotted lines) isotherms.

Table 2. Heat of Adsorption (kcal/mol): Experimental vs. Simulated Results

	Na-Y	Ag-Y	H-USY
Benzene	17.7–18.2	20.5–20.7	6.2–7.2
Experimental	16.4–18.5	18.8–21.1	8.2–9.2
Monte Carlo simulation	—	17.2	—
Molecular orbital calculation	17.5–18.0	—	—
Barthomeuf et al.*			
Cyclohexane	10.9–13.0	12.1–12.3	4.1–4.3
Experimental	12.0–13.2	—	—
Barthomeuf et al.*			

*Barthomeuf and Ha, 1973.

isosteric heat of adsorption of benzene was slightly higher than that of cyclohexane. A possible reason for the higher heat of benzene adsorption was the existence of H^+ in the zeolite, although the number of protons was extremely small (less than one per unit cell). The interaction between protons in zeolite and π-electrons of benzene might be stronger than the interaction between oxygen in zeolite and benzene. Therefore, the amounts of benzene adsorption were slightly larger than that of cyclohexane at less than 0.04 atm, leading to its higher heat of adsorption.

On all other sorbents investigated in this work, larger amounts of benzene were adsorbed at all pressure ranges. Heats of adsorption for benzene were 18 kcal/mol for Na-Y and 21 kcal/mol for Ag-Y, while heats of adsorption for cyclohexane were 10–12 kcal/mol for both Na-Y and Ag-Y. These results are clearly due to the strong interactions between the cations in zeolite and the benzene molecule. Consequently, Ag-Y and Na-Y could adsorb large amounts of benzene even at a pressure of less than 0.01 atm. The heats of adsorption on Na-Y were comparable to previous work (Barthomeuf and Ha, 1973). Most importantly, Ag-Y showed the strongest interactions for benzene and the highest heats of adsorption (20.5 kcal/mol). For cyclohexane adsorption, the adsorption amounts and heat of adsorption were almost the same between Ag-Y and Na-Y, since π-complexation was absent for cyclohexane. A detailed discussion will be made in the section of molecular orbital calculation and Monte Carlo simulation results. These results indicated that improved purification performance of benzene from cyclohexane is possible using Ag-Y. The isotherms of both Ag-Y and Na-Y are reversible, although it took a little longer time to desorb benzene and cyclohexane. For example, 200 min are necessary to desorb benzene completely after the adsorption at 0.1 atm. This slow desorption is clearly due to the strong interaction between benzene and Ag. However, the bonds are of the order of 20 kcal/mol, which are weak enough so a substantial fraction of the adsorbed benzene is desorbed in a few minutes. For practical applications, thermal desorption may be a desirable option.

Pd-Y gave lower adsorption amounts than both Ag-Y and Na-Y. This decrease of adsorption amounts by ion-exchange with Pd was due to degradation of the zeolite structure. In Figure 5, the pore-size distributions for all sorbents calculated from N_2 isotherms at 77 K are shown. Pd-Y had a small pore volume with a wide pore-size distribution, clearly indicating the collapse of the zeolite pore structure or pore blockage by Pd. The Pd ion exchange was performed at 80°C,

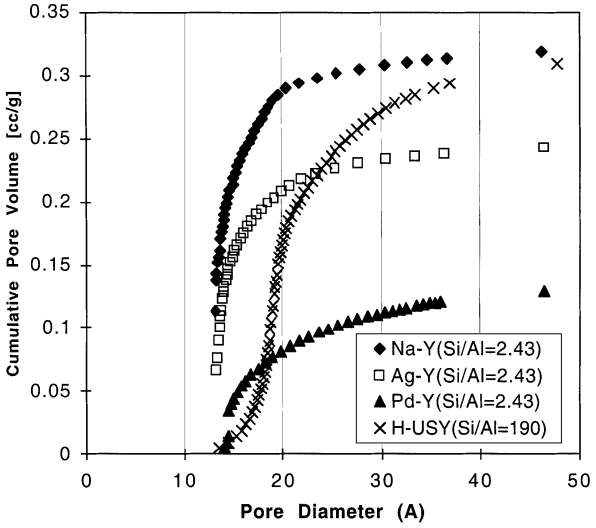

Figure 5. Pore-size distributions of Na-Y, Ag-Y, Pd-Y, and H-USY.

compared with the Ag ion exchange at room temperature. A collapsing zeolite structure tends to occur considerably more in acidic solution and at higher temperatures. The pore volume of Ag-Y also decreased by 23% after ion exchange. However, this reduction of Ag-Y was mainly caused by 37% density increase of the zeolite lattice by replacing Na^+ with Ag^+ (27% reduction of pore volume per weight basis). The pore structure of Ag-Y was intact after ion exchange.

Another interesting phenomenon in Figure 5 is the apparent shift of the pore-size distribution in H-USY toward a higher value, compared to other zeolites. This was likely due to the lower polarizability of oxygen in the framework of high-SiO_2 zeolites (Pellenq and Nicholson, 1993), which will be discussed in detail in the subsection of Monte Carlo simulation results. Otherwise, the interactions between nitrogen and cations in zeolites would have led to a shift of the pore sizes toward smaller values for Na-Y, Ag-Y, and Pd-Y. Since the pore sizes of Na-Y, Ag-Y, and Pd-Y were the same as the actual value for Y zeolites (1.3 nm), the latter explanation is not plausible.

Separation Factors. The pure-component adsorption data were first fitted by both Dubinin–Astakhov (D–A) and Langmuir–Freundlich (L–F) isotherms. The separation factors of benzene over cyclohexane were then obtained using the equivalent multicomponent isotherms. In the D–A equation of pure-component gas, the volume adsorbed, V, at relative pressures P/P_s is expressed as

$$V = V_0 \exp\left[-\left(C \ln \frac{P_s}{P}\right)^n\right], \tag{10}$$

where

$$C = \frac{RT}{\beta E_0}. \tag{11}$$

Doong and Yang (1988) extended the D–A equation to mixed-gas adsorption in a simple way by using the concept of maximum available pore volume without any additional equations such as the Lewis relationship (Lewis et al., 1950). For binary mixtures,

$$V_1 = (V_{01} - V_2) \exp\left[-\left(C_1 \ln \frac{P_{s1}}{P_1}\right)^{n_1}\right] \tag{12}$$

$$V_2 = (V_{02} - V_1) \exp\left[-\left(C_2 \ln \frac{P_{s2}}{P_2}\right)^{n_2}\right]. \tag{13}$$

Since Eqs. 12 and 13 are linear, V_1 and V_2 can be obtained in a straightforward fashion. After the calculation of V_1 and V_2, volumetric adsorbed amounts were converted to molar adsorbed amounts and the separation factors were calculated. The conversion of molar adsorbed amount to volumetric adsorbed amount and vice versa was performed using the liquid density data of the adsorbates. The liquid density at 120 and 180°C were obtained by the modified Rackett equation by Spencer and Adler (1978). The liquid densities used in this work were 0.769 g/cm^3 at 120°C and 0.689 g/cm^3 at 180°C for benzene, and 0.679 g/cm^3 at 120°C and 0.606 g/cm^3 at

Table 3. Parameters for D–A and L–F Equations

			D–A Equation				L–F Equation		
Adsorbent	Adsorbate	Temp. (°C)	V_o (cm^3/g)	C	n	Ps (atm)	q_o (mmol/g)	B (1/atm)	n
Na-Y	Benzene	120	0.295	0.092	3.76	2.96	3.15	30.7	2.53
	Benzene	180	0.326	0.120	4.73	10.07	2.82	449	0.9
	Cyclohexane	120	0.267	0.149	5.01	2.84	2.58	51.2	1.18
	Cyclohexane	180	0.264	0.168	6.44	9.48	2.30	61.9	0.77
Ag-Y	Benzene	120	0.244	0.056	1.57	2.96	3.07	3.67	7.46
	Benzene	180	0.248	0.082	3.05	10.07	2.03	156	1.85
	Cyclohexane	120	0.225	0.133	4.32	2.84	2.02	48.4	1.44
	Cyclohexane	180	0.237	0.145	4.96	9.48	1.80	74.3	0.91
H-USY	Benzene	120	0.237	0.318	2.84	2.96	3.40	11.2	0.62
	Benzene	180	0.234	0.333	2.17	10.07	3.40	1.11	0.74
	Cyclohexane	120	0.249	0.265	5.85	2.84	1.33	2500000	0.2
	Cyclohexane	180	0.15	0.232	4.93	9.48	0.73	260	0.39
Pd-Y	Benzene	120	0.173	0.237	2.15	2.96	0.883	240	0.7
	Cyclohexane	120	0.16	0.317	1.34	2.84	0.753	9.22	1.2

Table 4. Separation Factors Estimated by the D–A and L–F Equations

Press (atm)		Temp.	D–A Equation		L–F Equation	
Benzene	Cyclohexane	(°C)	Ag-Y	Na-Y	Ag-Y	Na-Y
0.01	1	120	107	—	6	12
0.001	1	120	416	441	45	48
0.0001	1	120	2,286	1,016	335	191
0.00001	1	120	14,361	2,553	2,462	767
0.01	1	180	39	95	19	5.4
0.001	1	180	120	71	57	4.2
0.0001	1	180	456	26	163	3.3
0.00001	1	180	1,767	0.5	470	2.6

180°C for cyclohexane. The adsorbed molar volumes were assumed to be the same in both single- and mixed-gas adsorption.

For the L–F isotherm equation, the pure-component isotherm is written using three adjustable parameters:

$$q = \frac{q_0 B P^{1/n}}{1 + B P^{1/n}}. \tag{14}$$

The L–F equation also can be extended for an n-component mixture (Yang, 1987):

$$q_i = \frac{q_0 B_i P_i^{1/ni}}{1 + \sum_{j=1}^{n} B_j P_j^{1/nj}}. \tag{15}$$

The fitting parameters for both isotherms are listed in Table 3, and the fitted curves are plotted in Figures 1–4. The separation factors of benzene over cyclohexane were calculated using the equilibrium mole fractions in adsorbed and gas phases:

$$\alpha = \frac{X_{\text{benzene}}/Y_{\text{benzene}}}{X_{\text{cyclohexane}}/Y_{\text{cyclohexane}}}. \tag{16}$$

The calculated separation factors for Ag-Y and Na-Y are compared in Table 4. Both D–A and L–F equations led to a similar dependence of the separation factor on pressure. The separation factor for Ag-Y increased with decreasing concentration of benzene, while that for Na-Y at 180°C decreased. Although the separation factors calculated by the two isotherms were not the same, the advantages of Ag-Y over Na-Y are clearly seen, especially at lower concentrations of benzene. This is certainly because Ag-Y can maintain its adsorption ability to benzene, even at around 1×10^{-5} atm. On the other hand, at 0.01 and 0.001 atm of benzene and at the lower temperature of 120°C, Na-Y showed equivalent separation factors to Ag-Y.

For separations by adsorption and membranes, a separation factor on the order of 10 is considered high. For example, in air separation by pressure swing adsorption using zeolites and also by polymeric membranes, systems with separation factors (N_2/O_2 for adsorption and O_2/N_2 for membranes) of near 10 are commercially used. For aromatics/aliphatics separations using liquid membranes (e.g., toluene/heptane and benzene/heptane separations), separation factors on the order of 10–100 yielded excellent separations (Li, 1968, 1971). The separation factors shown in Table 4, on the order of 10–10,000, are excellent for separation/purification.

Diffusion Time Constants. In Table 5, diffusion time constants calculated from 0–0.3 fractional uptake were summarized. The diffusion time constants of benzene and cyclohexane in Na-Y and Ag-Y were on the order of 10^{-4} L/s. These values were almost the same as those of benzene and cyclohexane into $AgNO_3$ monolayer dispersed SiO_2 sorbent (Takahashi et al.). However, these values were an order of magnitude lower than those of propylene and propane in $AgNO_3$ monolayer-dispersed SiO_2 sorbent (Rege, 1998) and at least the same as those of ethylene and ethane into Ag

Table 5. Diffusion Time Constants of Benzene and Cyclohexane

Adsorbents	Temp. (°C)	Benzene (1/s)	(Pres. Change) (atm)	Cylohexane (1/s)	(Pres. Change) (atm)
Na-Y	120	2.1×10^{-4}	$(5.4\times10^{-3}$–$2.6\times10^{-2})$	9.8×10^{-4}	$(1.1\times10^{-2}$–$2.0\times10^{-2})$
Ag-Y	120	4.2×10^{-4}	$(5.4\times10^{-3}$–$2.6\times10^{-2})$	1.1×10^{-4}	$(1.1\times10^{-2}$–$2.0\times10^{-2})$
$AgNO_3/SiO_2$(0.33 g/g)*	120	1.3×10^{-4}	$(2.0\times10^{-3}$–$3.7\times10^{-2})$	2.9×10^{-4}	$(2.0\times10^{-3}$–$3.7\times10^{-2})$
Adsorbents	Temp. (°C)	Propylene (1/s)	(Pres. Change) (atm)	Propane (1/s)	(Press. Change) (atm)
$AgNO_3/SiO_2$(0.33 g/g)**	70	3.5×10^{-3}	(0–1)	—	—
Ag-Amberlyst-35†	70	1.5×10^{-4}	—	1.4×10^{-4}	—

*Takahashi et al., 2000.
**Rege et al., 1998.
†Wu et al., 1997.

ion-exchanged resins (Wu et al., 1997). The diffusion rates of benzene in these zeolites are high for applications (Yang, 1987).

Molecular orbital calculation

Adsorption Bond Energy and Molecular Geometries. Adsorption energy and structural geometry were calculated using molecular orbital theory. The calculated heat of adsorption using the B3LYP/3-21G level by Eq. 1 is also compared with experimental and Monte Carlo simulation results in Table 2. The theoretical value, 17.2 kcal/mol, was in fairly good agreement with the experimental value. The comparison of bond length by benzene adsorption revealed that the Ag-O length increased from 3.023 Å to 3.246 Å. The C–C bond length in benzene also increased from 1.385 Å to 1.385–1.391 Å. This trend was consistent with that for benzene interaction with AgCl (Takahashi et al.).

Natural Bond Orbital Results. The nature of benzene–Ag zeolite interaction can be better understood by analyzing the NBO results. The main feature of the interaction can be seen from the population changes in the vacant outer-shell s-orbital of the silver and those in the d-orbitals of silver upon adsorption. In Table 6, the NBO analysis results for benzene on Ag zeolite are compared with other combinations of adsorbates and adsorbents. According to the electron population changes by benzene adsorption on Ag zeolite, the trend is in agreement with the previously reported π-complexation trend (Cheng, 1996; Huang et al., 1999a,b,c; Takahashi et al., 2000), that is, donation of electron charges from the p-orbitals of benzene to the vacant s-orbital of the silver (σ donation) and, simultaneously, back donation of electron charges from the d-orbitals of silver to the π^*-orbitals of benzene (d-π^* back donation). The contribution of d-π^* back donation is larger than σ donation, resulting in a decrease in the net electron charge in silver. The net electron charge of carbon in benzene increased instead.

The differences of electron population changes between benzene and ethylene adsorption deserve discussion. From Table 6, it is seen that the contribution of σ donation is predominant in ethylene adsorption, while d-π^* back donation is slightly larger in benzene adsorption. Also, the extent of σ donation and d-π^* back donation by benzene adsorption was considerably smaller compared with ethylene adsorption. Therefore, α-complexation with benzene was weaker than that with ethylene. Weak π-complexation of benzene can also be understood by the difference in bond lengths. The bond length between carbon in ethylene and silver in AgCl was 2.66 Å (Huang et al., 1999b), while that between carbon in benzene and silver in Ag zeolite or AgCl was 2.71–3.7 Å or 3.22 Å (Takahashi et al., 2000), respectively. This longer bond length was caused by the smaller overlap of orbitals from the weaker π-complexation.

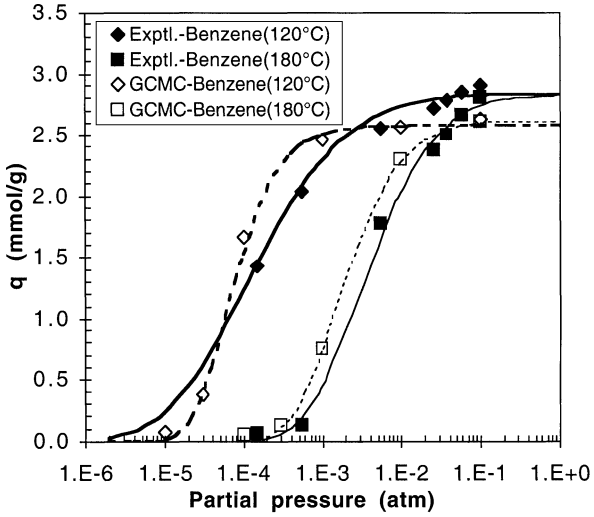

Figure 6. Comparison of experimental and GCMC simulation for adsorption of benzene on Na-Y.

Monte Carlo simulation

Monte Carlo simulation of adsorption isotherms provides great insight into the adsorption mechanism via model construction, charge assignment, and force field determination. In this section, benzene adsorption on Na-Y, H-USY, and Ag-Y is simulated, and the mechanism of adsorption on each zeolite is discussed.

Na-Y Zeolite. The GCMC simulation results of benzene isotherms at 120° and 180°C using the potential parameters given in Table 1 are shown in Figure 6, where they are also compared with experimental data. The simulation results were in excellent agreement with experimental data. The calculated heats of adsorption were 16.4–18.5 kcal/mol, which were in agreement with those from experiments. It was hence confirmed that the energy expressions and parameters were suitable for simulation of benzene isotherms on Na-Y.

H-USY Zeolite. First, simulation of benzene isotherms on H-USY was attempted using the same potential parameters

Table 6. NBO Analysis of π-Complexation: Electron Population Changes of Each Orbital after Adsorption

		Silver			Carbon		
	Method/BasisSet	5*S*	$\Sigma 4d$	Net Change	2*s*	$\Sigma 2p$	Net Change
Benzene on Ag Zeolite	B3LYP/3-21G	0.00541	−0.0135	−0.00805	0.00554	0.00709	0.01263
Benzene on AgCl*	B3LYP/LanL2DZ	0.0033	−0.0071	−0.0038	—	—	—
C_2H_4 on Ag Zeolite**	MP2/3-21G	0.0596	−0.0177	0.0419	0.0203	0.0193	0.0396
C_2H_4 on AgCl**	MP2/3-21G	0.1204	−0.0470	0.0734	0.0226	0.0142	0.0368
C_2H_4 on AgCl†	B3LYP/LanL2DZ	0.061	−0.055	0.006	—	—	—

*Takahashi et al., 2000.
**Chen and Yang, 1996.
†Huang et al., 1999a.

as on Na-Y. However, the simulated isotherms were considerably higher than the experimental data. This disagreement was caused by incorrect well-depth parameters, $\epsilon_{O\text{-}C}$ and $\epsilon_{O\text{-}H}$, for van der Waals interaction. Pellenq and Nicholson (1993) reported the values of the polarizabilities of framework atoms in silicalite and aluminosilicates determined from Auger electron spectroscopy data. It was found that the polarizability for oxygen in a zeolite framework is sensitive to the ratio of silicon to aluminum and also the nature of the extra framework cations. Watanabe et al. (1995) used different potential values for oxygen in silicalite (0.202 kcal/mol), denoted by Oz(Si-O-Si), and that in aluminosilicates (0.334 kcal/mol), denoted by Oz(Si-O-Al).

In this work, an adjustment of $\epsilon_{Oz(Si\text{-}O\text{-}Si)\text{-}C}$ and $\epsilon_{Oz(Si\text{-}O\text{-}Si)\text{-}H}$ was made to simulate the experimental Henry's law constants at 120° and 180°C. Here, since low-pressure data depend only on the benzene–zeolite interactions, the benzene–benzene interactions were neglected. Using the well-depth parameter for $\epsilon_{Na\text{-}C} = 0.04187$ kcal/mol and $\epsilon_{Na\text{-}H} = 0.03153$ kcal/mol for Na-Y (in Table 1) and assuming $\epsilon_{Na} = 0.041$ kcal/mol, as used by Watanabe et al. (1995) for Na-A and Na-X, $\epsilon_C = 0.0428$ kcal/mol and $\epsilon_H = 0.0243$ kcal/mol were obtained from the geometric combination rule, Eq. 9. Therefore, $\epsilon_{Oz(Si\text{-}O\text{-}Si)\text{-}C}$ and $\epsilon_{Oz(Si\text{-}O\text{-}Si)\text{-}H}$ for H-USY could be expressed as $(0.0428 \times \epsilon_{Oz(Si\text{-}O\text{-}Si)})^{0.5}$ and as $(0.0243 \times \epsilon_{Oz(Si\text{-}O\text{-}Si)})^{0.5}$, respectively. By fitting with $\epsilon_{Oz(Si\text{-}O\text{-}Si)}$, $\epsilon_{Oz(Si\text{-}O\text{-}Si)} = 0.655$ kcal/mol was obtained to fit the experimental Henry's law constant of 0.519 molecule/(cell·kPa) at 120°C and 0.137 molecule/(cell·kPa) at 180°C. The ratio of $\epsilon_{Oz(Si\text{-}O\text{-}Si)}$ over $\epsilon_{Oz(Si\text{-}O\text{-}Al)}$ was 0.44 (calculated from $\epsilon_{Oz(Si\text{-}O\text{-}Al)\text{-}H}$)–0.60 (calculated from $\epsilon_{Oz(Si\text{-}O\text{-}Al)\text{-}C}$), which was in agreement with the ratio of 0.60 obtained by Watanabe et al. (1995).

Using the modified parameters for H-USY (in Table 1), the benzene isotherms were calculated and compared with experimental isotherms in Figure 7. Again, the isotherms and the heat of adsorption (8.2–9.2 kcal/mol) obtained from simulation were in excellent agreement with the experimental data.

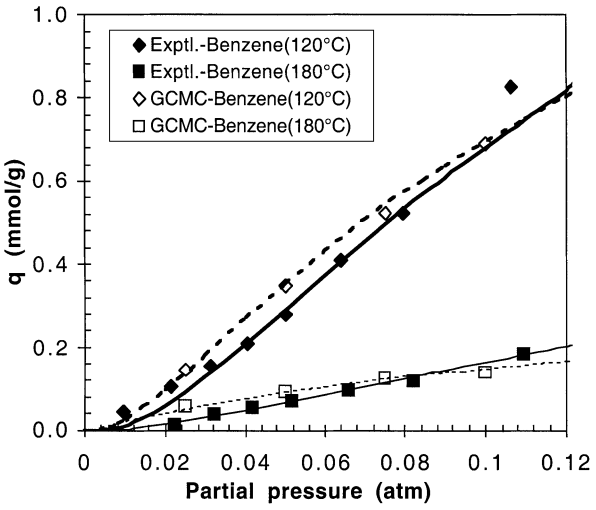

Figure 7. Comparison of experimental and GCMC simulation for adsorption of benzene on H-USY.

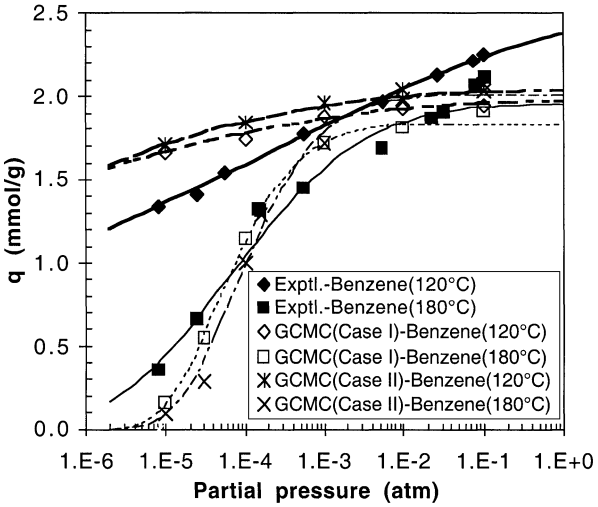

Figure 8. Comparison of experimental and GCMC simulation for adsorption of benzene on Ag-Y.

Ag-Y Zeolite. The potential parameters for Ag-Y are listed in Table 1. These parameters were modified to get the low pressure points of the isotherm at 180°C (1.30 mmol/g at 1.6×10^{-4} atm), although adjustment of the parameters to fit the experimental Henry's law constant was preferable. The reason not to use the experimental Henry's constant was that the small pressure values (8.7×10^{-6} atm) at the lowest adsorbed amount in the isotherms might lead to the large error of potential parameters. The procedure of adjustment was basically the same as in the case for H-USY, except for changing the ϵ_{Ag} value instead of the $\epsilon_{Oz(Si\text{-}O\text{-}Si)}$ value. $\epsilon_C = 0.0428$ kcal/mol and $\epsilon_H = 0.0243$ kcal/mol were obtained from the geometric combination rule (Eq. 9). Then, $\epsilon_{Ag\text{-}C}$ and $\epsilon_{Ag\text{-}H}$ for Ag-Y could be estimated from $(0.0428 \times \epsilon_{Ag})^{0.5}$ and $(0.0243 \times \epsilon_{Ag})^{0.5}$, respectively. In Case I for Ag-Y, ϵ_{Ag} became 14.3 kcal/mol, while $\epsilon_{Ag} = 13.5$ kcal/mol was obtained for Case II. The larger well-depth parameter was needed for Case I to compensate for the weaker Coulomb interaction due to the smaller Ag cation charge. In both cases, the ϵ_{Ag} values used were more than two orders of magnitude greater than ϵ_{Na}, clearly indicating the strong interaction from π-complexation.

Figure 8 shows the simulation results of benzene on Ag-Y for Case I and Case II. The differences between Case I and Case II were fairly small. In both cases, the agreement with experimental isotherms was not as good as that for Na-Y and H-USY. However, they certainly followed the basic trend of the experimental isotherms. The calculated heat of adsorption was 18.8–21.1 kcal/mol, which was higher than Na-Y and also in agreement with the experimental value.

In all cases, not only Ag-Y but also Na-Y and H-USY, with few exceptions, the simulated isotherms tended to be higher than the experimental isotherms in the lower pressure range, while they were lower in the higher pressure range. The higher simulation results at low pressures might be caused by the larger values for the well-depth parameter between oxygen (zeolite)–carbon (benzene) interaction and oxygen (zeolite)–hydrogen (benzene) interaction. The other possible cause was the imperfection of the zeolite crystals. Since zeo-

lites contain defects while in Monte Carlo simulation, a perfect zeolite lattice was assumed. In the high pressure range, larger experimental values were possibly caused by adsorption between zeolite crystals.

Adsorption sites for benzene on Na-Y and Ag-Y were investigated using the Mass Cloud Plots function in Cerius2 (not shown here). It was confirmed that benzene was adsorbed preferentially near the SII cation sites and the center of the 12-ring window, which was consistent with the neutron diffraction data for Na-Y obtained by Fitch (1986). For Ag-Y, benzene was adsorbed slightly further away from the SII cation sites than that in Na-Y, due to the fact that the van der Waals radius of Ag^+ is 30% larger than that of Na^+.

Acknowledgments

This work was supported by the National Science Foundation under Grant CTS-9819008. We are grateful to NGK Insulators, Ltd., Nagoya, Japan, for financial support to A.T. during his time at the University of Michigan. We also thank Dr. Frances Yang for teaching the molecular orbital calculation methodology to A.T.

Notation

A = repulsive parameter for Buckingham potential
B = repulsive parameter for Buckingham potential or Langmuir constant
C = dispersive parameter for Buckingham potential or constant for D-A equation
D = diffusivity
E = energy
n = constant
P = pressure
q = point charge or molar adsorbed amount
R = van der Waals radii or gas constant
r = distance or radius
T = temperature
U = potential energy
V = volumetric adsorbed amount
X = equilibrium mole fraction in adsorbed phase
Y = equilibrium mole fraction in gas phase

Greek letters

α = polarizability or separation factor
β = adjustable parameter
ϵ = well depth parameter for Lennard-Jones potential
σ = distance parameter for Lennard-Jones potential

Subscripts

i = atom site or component
j = atom site or component
s = saturation

Literature Cited

Allen, M. P., and D. J. Tildesley, *Computer Simulation of Liquid*, Clarendon, Oxford (1987).

Atwood, J. L., "New Inclusion Methods for Separations Problems," *Sep. Sci. Technol.*, **19**, 751 (1984).

Bailes, P. J., "Petroleum and Petrochemicals Processing—Introduction and Aromatics-Aliphatics Separation," *Handbook of Solvent Extraction*, T. C. Lo, M. H. I. Baird, and C. Hansen, eds., Wiley, New York, p. 517 (1983).

Barthomeuf, D., and B.-H. Ha, "Adsorption of Benzene and Cyclohexane on Faujasite-Type Zeolites," *J. Chem. Soc. Faraday Trans.*, **69**, 2147 (1973).

Becke, A. D., "Density-Functional Thermochemistry: II. The Effect of the Perdew-Wang Generalized-Gradient Correlation Correction," *J. Chem. Phys.*, **97**, 9173 (1992).

Becke, A. D., "Density Functional Thermochemistry: III. The Role of Exact Exchanges," *J. Chem. Phys.*, **98**, 5648 (1993a).

Becke, A. D., "A New Mixing of Hartree-Fock and Local Density-Functional Theories," *J. Chem. Phys.*, **98**, 1372 (1993b).

Blytas, G. C., "Separation of Unsaturates by Complexing with Nonaqueous Solutions of Cuprous Salts," *Separation and Purification Technology*, N. N. Li and J. M. Calo, eds., Chap. 2, Dekker, New York (1992).

Bowie, J. E., *Data Visualization in Molecular Science: Tools for Insight and Innovation*, Chap. 9, Addison-Wesley, Reading, MA (1995).

Breck, D. W., *Zeolite Molecular Sieves: Structure, Chemistry and Use*, Wiley, New York (1974).

Chen, N., and R. T. Yang, "*Ab Initio* Molecular Orbital Study of Adsorption of Oxygen, Nitrogen, and Ethylene on Silver-Zeolite and Silver Halides," *Ind. Eng. Chem. Res.*, **35**, 4020 (1996).

Cheng, L. S., and R. T. Yang, "Improved Horvath-Kawazoe Equations Including Spherical Pore Models for Calculating Micropore Size Distribution," *Chem. Eng. Sci.*, **49**, 2599 (1994).

Cheng, L. S., and R. T. Yang, "Monolayer Cuprous Chloride Dispersed on Pillared Clays for Olefin-Paraffin Separation by π-Complexation," *Adsorption*, **1**, 61 (1995).

Cotton, F. A., and G. Wilkinson, *Advanced Inorganic Chemistry*, 2nd ed., chaps. 25 and 28, Interscience, New York (1966).

Demontis, P., S. Yashonath, and M. L. Klein, "Localization and Mobility of Benzene in Sodium-Y Zeolite by Molecular Dynamics Calculations," *J. Phys. Chem.*, **93**, 5016 (1989).

Doong, S. J., and R. T. Yang, "A Simple Potential-Theory Model for Predicting Mixed-Gas Adsorption," *Ind. Eng. Chem. Res.*, **27**, 630 (1988).

Eldridge, R. B., "Olefin/Paraffin Separation Technology: Review," *Ind. Eng. Chem. Res.*, **32**, 2208 (1993).

Fitch, A. N., H. Jobic, and A. Renourez, "A Localization of Benzene in Sodium-Y Zeolite by Neutron Diffraction," *J. Phys. Chem.*, **90**, 1311 (1986).

Frisch, M. J., G. W. Trucks, H. B. Schlegel, P. M. W. Gill, B. G. Johnson, M. A. Robs, J. R. Cheeseman, T. Keith, G. Petersson, J. A. Montgomery, K. Raghavachari, M. A. Al-Laham, V. G. Zakrzewski, J. V. Ortiz, J. B. Foresman, C. Y. Peng, P. Y. Ayala, W. Chen, M. W. Wong, J. L. Andres, E. S. Replogle, R. Gomperts, R. L. Martin, D. J. Fox, J. S. Binkley, D. J. DeFrees, J. Baker, J. P. Stewart, M. Head-Gordon, C. Gonzalez, and J. A. Pople, *Gaussian 94*, Rev. B.3, Gaussian, Inc., Pittsburgh, PA (1995).

Glendening, E. D., A. E. Reed, J. E. Carpenter, and F. Weinhold, *NBO Version 3.1* (1995).

Hao, J., T. Tanaka, H. Kita, and K. Okamoto, "The Pervaporation Properties of Sulfonyl-Containing Polyimide Membranes to Aromatic/Aliphatic Hydrocarbon Mixture," *J. Membr. Sci.*, **132**, 97 (1997).

Ho, W. S., G. Doyle, D. W. Savage, and R. L. Pruett, "Olefin Separation via Complexation with Cuprous Diketonate," *Ind. Eng. Chem. Res.*, **27**, 334 (1988).

Horvath, G., and K. Kawazoe, "Method for Calculation of Effective Pore Size Distribution in Molecular Sieve Carbon," *J. Chem. Eng. Jpn.*, **16**, 470 (1983).

Huang, H. Y., J. Padin, and R. T. Yang, "Anion and Cation Effects on Olefin Adsorption on Silver and Copper Halides: *Ab Initio* Effective Core Potential Study of π-Complexation," *J. Phys. Chem. B*, **103**, 3206 (1999a).

Huang, H. Y., J. Padin, and R. T. Yang, "Comparison of π-Complexations of Ethylene and Carbon Monoxide with Cu^+ and Ag^+," *Ind. Eng. Chem. Res.*, **38**, 2720 (1999b).

Huang, H. Y., R. T. Yang, and N. Chen, "Anion Effects on the Adsorption of Acetylene by Nickel Halides," *Langmuir*, **15**, 7647 (1999c).

Hutson, N. D., B. A. Reisner, R. T. Yang, and B. H. Toby, "Silver Ion-Exchanged Zeolites Y, X and Low Silica X: Observations of Thermally Induced Cation/Cluster Migration and the Resulting Effects on Equilibrium Adsorption of Nitrogen," *Chem. Mater.*, **12**, 3020 (2000).

Jeanneret, J. J., "UOP Sulfolane Process," *Handbook of Petroleum Refining Process*, R. A. Meyers, ed., McGraw-Hill, New York, p. 2.13 (1997).

Keller, G. E., A. E. Marcinkowsky, S. K. Verma, and K. D. Williamson, "Olefin Recovery and Purification via Silver Complex-

ation," *Separation and Purification Technology*, N. N. Li and J. M. Calo, eds., Dekker, New York, p. 59 (1992).
King, C. J., "Separation Process Based on Reversible Chemical Complexation," Handbook of Separation Process Technology, R. W. Rousseau, ed., Wiley, New York (1987).
Kitagawa, T., T. Tsunekawa, and K. Iwayama, "Monte Carlo Simulation on Adsorption of Benzene and Xylene in Sodium-Y Zeolites," *Microporous Mater.*, **7**, 227 (1996).
Klemm, E., J. Wang, and G. A. Emig, "Comparative Study of the Sorption of Benzene and Phenol in Silicalite, HAlZSM-5 and NaAlZSM-5 by Computer Simulation," *Microporous Mater.*, **26**, 11 (1998).
Kravias, F., and A. L. Myers, "Monte Carlo Simulation of Adsorption of Non-Polar and Polar Molecules in Zeolite X," *Mol. Sim.*, **8**, 23 (1991).
Laboy, M. M., I. Santiago, and G. E. Lopez, "Computing Adsorption Isotherms for Benzene, Toluene, and p-Xylene in Heulandite Zeolite," *Ind. Eng. Chem. Res.*, **38**, 4938 (1999).
Lee, C., W. Yang, and R. G. Parr, "Development of the Colle-Salvetti Correlation-Energy Formula into a Functional of the Electron Density," *Phys. Rev.*, **B37**, 785 (1988).
Lewis, W. K., E. R. Gilliland, B. Chertow, and W. P. Cadogan, "Adsorption Equilibria-Hydrocarbon Gas Mixtures," *Ind. Eng. Chem.*, **42**, 1319 (1950).
Li, N. N., "Separating Hydrocarbons with Liquid Membranes," U.S. Patent 3,410,794 (1968).
Li, N. N., "Separation of Hydrocarbons by Liquid Membrane Permeation," *Ind. Eng. Chem. Process Des. Dev.*, **10**, 215 (1971).
Li, Y., and J. N. Armor, "Catalytic Combustion of Methane over Palladium Exchanged Zeolites," *Appl. Catal.*, **B3**, 275 (1994).
Matz, M. J., and K. S. Knaebel, "Criteria for Selection of an Adsorption for a Temperature Swing Process: Applied to Purification of an Aliphatic Solvent Contaminated with Aromatics Solutes," *Sep. Sci. Technol.*, **25**, 961 (1990).
Molecular Simulation Inc., *Cerius2 Property Prediction*, Release 3.8 (September 1998).
O'Malley, P. J., and C. J. Braithwaite, "*Ab Initio* Molecular Orbital and Molecular Graphics Studies of Benzene Adsorption in NaY Zeolite," *Zeolites*, **15**, 198 (1995).
Padin, J., and R. T. Yang, "Tailoring New Adsorbents Based on π-Complexation: Cation and Substrate Effects on Selective Acetylene Adsorption," *Ind. Eng. Chem. Res.*, **36**, 4224 (1997).
Padin, J., R. T. Yang, and C. L. Munson, "New Sorbents for Olefin/Paraffin Separations and Olefin Purification for C_4 Hydrocarbons," *Ind. Eng. Chem. Res.*, **38**, 3614 (1999).
Padin, J., and R. T. Yang, "New Sorbents for Olefin-Paraffin Separation by Adsorption via π-Complexation: I. Synthesis and Effects of Anions and Substrates," *Chem. Eng. Sci.*, **55**, 2607 (2000).
Pellenq, R. J.-M., and D. Nicholson, "In-Framework Ion Dipole Polarizabilities in Non-Porous and Porous Silicalites and Aluminosilicates, Determined from Auger Electron Spectroscopy Data," *J. Chem. Soc. Faraday Trans.*, **89**, 2499 (1993).
Quinn, H. W., "Hydrocarbon Separations with Silver(I) Systems," *Progress in Separation and Purification*, Vol. 4, E. S. Perry, ed., Interscience, New York (1971).
Rappe, A. K., and W. A. Goddard III, "Charge Equilibrium for Molecular Dynamics Simulations," *J. Phys. Chem.*, **95**, 3358 (1991).
Razmus, D. M., and C. K. Hall, "Prediction of Gas Adsorption in 5 Azeolites Using Monte Carlo Simulation," *AIChE J.*, **37**, 769 (1991).
Reed, A. E., R. B. Weinstock, and F. Weinhold, "Natural Population Analysis," *J. Chem. Phys.*, **83**(2), 735 (1985).
Rege, S. U., J. Padin, and R. T. Yang, "Olefin-Paraffin Separation by Adsorption: Equilibrium Separation by π-Complexation vs. Kinetic Separation," *AIChE J.*, **44**, 799 (1998).
Safarik, D. J., and R. B. Eldridge, "Olefin/Paraffin Separations by Reactive Adsorption: A Review," *Ind. Eng. Chem. Res.*, **37**, 2571 (1998).
Snurr, R. Q., A. T. Bell, and D. N. Theodorou, "A Hierarchical Atomistic/Lattice Simulation Approach for the Prediction of Adsorption Thermodynamics of Benzene in Silicalite," *J. Phys. Chem.*, **98**, 5111 (1994).
Spencer, C. F., and S. B. Adler, "A Critical Review of Equations for Predicting Saturated Liquid Density," *J. Chem. Eng. Data*, **23**, 82 (1978).
Takahashi, A., F. H. Yang, and R. T. Yang, "Aromatics/Aliphatics Separation by Adsorption: New Sorbent for Selective Aromatics Adsorption by π-Complexation," *Ind. Eng. Chem. Res.*, **39**, 3856 (2000).
Viruera-Martin, P., C. M. Zicovich-Wilson, and A. Corma, "*Ab Initio* Molecular Orbital Calculations of the Protonation Reaction of Propylene and Isobutene by Acidic OH Groups of Isomorphously Substituted Zeolites," *J. Phys. Chem.*, **97**, 13713 (1993).
Watanabe, K., N. Austin, and M. R. Stapleton, "Investigation of the Air Separation Properties of Zeolites types A, X and Y by Monte Carlo Simulations," *Mol. Sim.*, **15**, 197 (1995).
Williams, D. E., and S. R. Cox, "Nonbonded Potential for Azahydrocarbons: The Importance of the Coulombic Interaction," *Acta Crystallogr.*, **B40**, 404 (1984).
Woods, G. B., and J. S. Rowlinson, "Computer Simulation of Fluids in Zeolite X and Y," *J. Chem. Soc., Faraday Trans.*, **85**, 765 (1989).
Wu, Z., S. S. Han, S. H. Cho, J. N. Kim, K. T. Chue, and R. T. Yang, "Modification of Resin-Type Adsorbents for Ethane/Ethylene Separation," *Ind. Eng. Chem. Res.*, **36**, 2749 (1997).
Yang, R. T., *Gas Separation by Adsorption Processes*, Butterworth, Boston (1987) [reprinted (in paperback) by Imperial College Press, London (1997)].
Yang, R. T., and E. S. Kikkinides, "New Sorbents for Olefin/Paraffin Separations by Adsorption via π-Complexation," *AIChE J.*, **41**, 509 (1995).
Yeh, Y. T., "Diffusion and Adsorption of Gases in Molecular Sieves," PhD Diss., Univ. of New York at Buffalo, Buffalo, NY (1989).

Manuscript received Sept. 7, 2000, and revision received Jan. 22, 2002.